IOP PUBLISHING JOURNAL OF OPTICS
J. Opt. **14** (2012) 114001 (9pp) doi:10.1088/2040-8978/14/11/114001

Reconfigurable split rings based on MEMS switches and their application to tunable filters

David Bouyge[1,2], Aurelian Crunteanu[2], Miguel Durán-Sindreu[1], Arnaud Pothier[2], Pierre Blondy[2], Jordi Bonache[1], J Christophe Orlianges[3] and Ferran Martín[1]

[1] CIMITEC, Departament d'Enginyeria Electrònica, Universitat Autònoma de Barcelona, E-08193 Bellaterra (Barcelona), Spain
[2] MINACOM, XLIM–UMR CNRS 6172, University of Limoges, F-87000 Limoges, France
[3] SPCTS–UMR CNRS 6638, University of Limoges, F-87000 Limoges, France

E-mail: Pierre.blondy@xlim.fr, jean-christophe.orlianges@unilim.fr and Ferran.Martin@uab.es

Received 22 December 2011, accepted for publication 15 February 2012
Published 27 July 2012
Online at stacks.iop.org/JOpt/14/114001

Abstract
It is shown that radiofrequency micro-electromechanical-system (RF-MEMS) switches are useful to implement electronically reconfigurable split ring resonators (SRRs). Three different combinations of cantilever-type ON/OFF capacitive switches with SRRs are studied for the design of tunable or switchable SRR-loaded metamaterial transmission lines. These structures are then applied to the design of reconfigurable band stop and band pass filters at the X-frequency band. Through electrostatic actuation of the switches, the resonance frequency of SRRs can be shifted and, as a result, filter bandwidth and/or central frequency can be digitally controlled. Good agreement between theory and experiment is achieved.

Keywords: split ring resonators, RF-MEMS switches, metamaterials, tunable filters

(Some figures may appear in colour only in the online journal)

1. Introduction

The synthesis of switchable and reconfigurable metamaterials has been a subject of interest in recent years for their potential to tune the electromagnetic or optical properties of artificial structures based on them. In the microwave and radiofrequency domains, many metamaterials and metamaterial-based or -inspired structures and devices have been implemented by means of split ring resonators (SRRs) [1, 2], or by means of other electrically small resonators, such as complementary split ring resonators (CSRRs) [3, 4], spiral resonators [5–8], multiconductor SRRs [7, 8], chiral resonators [9, 10], open SRRs [11], open CSRRs [12], capacitive-loaded loops (CLLs) [13], etc. Therefore, the most straightforward approach to implement switchable and reconfigurable microwave metamaterials is to provide electronic tunability to the above-mentioned resonators.

Recently, tunability has been achieved by electric (or even by temperature) actuation in SRRs based on ferroelectric materials [14, 15] or vanadium dioxide [16]. It has also been shown that the electromagnetic response of SRRs can be tuned or switched by means of photoconductive substrates (prototypes operating at sub-millimeter wave and THz frequencies have been reported [17–19]). However, in the microwave region, tunable SRRs have generally been implemented by the addition of active semiconductor components, such as varactor diodes. By placing varactor diodes between the inner and the outer rings of the SRR, some of the authors proposed the synthesis of tunable metamaterial transmission lines and their application to the design of reconfigurable filters [20, 21]. The resulting particle, called a varactor-loaded split ring resonator (VLSRR), was also subsequently used by other authors to realize compact tunable notch filters and resonators [22, 23]. There was also pointed out by Aydin *et al* [24] the possibility to locate the variable

capacitance in the gap region of each SRR ring. These types of resonators have recently been applied to the implementation of metamaterial slabs with switchable permeability, which have been used to locally increase the signal-to-noise ratio in magnetic resonance imaging systems [25].

Tunable artificial transmission lines have also been implemented by means of varactor-loaded complementary split ring resonators (VLCSRR). Specifically, it was demonstrated by Velez *et al* [26] that microstrip lines loaded with VLCSRRs (etched in the ground plane) exhibit a tunable rejection band that can be attributed to a variation of the effective permittivity of the structure caused by a displacement of the resonance frequency of the particle. Moreover, it was also demonstrated that this rejection band can be switched to a left-handed and tunable pass band by merely etching gaps in the conductor strip, on top of the VLCSRR positions.

This kind of varactor-loaded particle can be very useful for manufacturing tunable metamaterials and related components in the L and S frequency bands (roughly covering the interval 2–4 GHz, according to the IEEE standard for radio waves). At higher frequencies, the dimensions of varactor diodes are too large. Furthermore, the performance of varactor-based tunable microwave systems is generally limited by losses, power consumption and nonlinearity. In this context, successful integration of RF-MEMS switches in SRRs (or in other electrically small resonators) is expected to be an enabling technology for many microwave applications (including the synthesis of metamaterials and devices based on them), thanks to their low loss, near-zero power dissipation, compactness and high linearity in broad frequency bands. RF-MEMS are still limited by reliability issues and moderate switching time, but recent progress has been done on these specific aspects [27–29]. The ability of this technology has been demonstrated over the past few years to provide an efficient solution to the tuning of microwave circuits [30, 31]. For that which concerns the implementation of metamaterial structures by combining RF-MEMS and split rings, the pioneering work is due to Gil *et al* [32], who realized a tunable stop band filter operating at the Q-band by periodically etching CSRRs in the central strip of a coplanar waveguide structure loaded with RF-MEMS variable capacitors on top of them, and to Hand and Cummer [33], who implemented single-loop split rings with MEMS switches integrated on them (similar to the varactor loading reported in [20, 21, 24]). Recently, MEMS-based tunable metamaterials at THz frequencies have been reported [34], where reconfigurability is achieved by mechanically reorienting micro-fabricated resonators (this approach is similar to that reported in [35] by the authors).

The originality of this work concerns the novel considered combinations of SRRs and cantilever-type RF-MEMS switches to achieve tunable or switchable electromagnetic responses in such resonators. The possibilities of the reported reconfigurable MEMS-based SRRs are illustrated through several prototypes implemented in microstrip technology, and specifically designed to behave as digitally tunable stop band and band pass filters at the X-band (8–12 GHz).

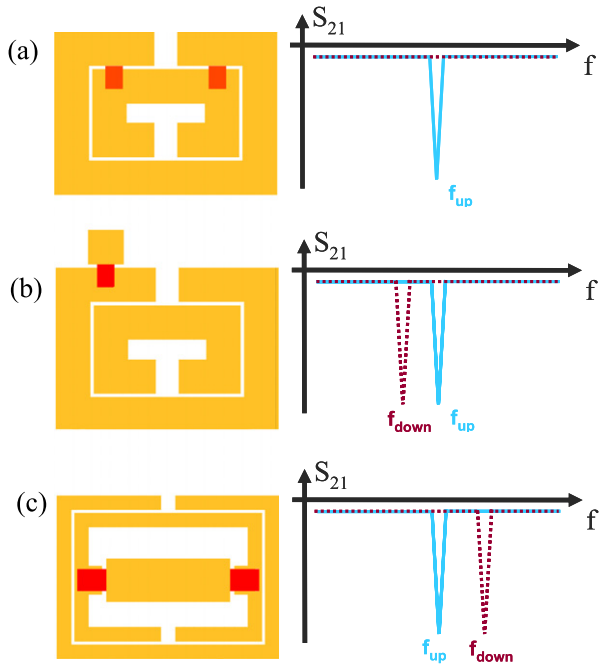

Figure 1. Illustration of cantilever-type RF-MEMS capacitive switches (represented by red rectangles) integration in SRRs for configurations I (a), II (b) and III (c). The typical frequency responses of the tunable resonators coupled to a transmission line when all switches are at the up state (blue curves) and when all switches are at the down state (red curves) are also depicted. At the SRR resonance frequency the particle is excited and the injected power is reflected back to the source, giving a notch in the transmission coefficient S_{21} at that frequency.

2. RF-MEMS-loaded SRRs: topologies, tuning principle and fabrication

The typical topology of a SRR consists of a pair of concentric metallic rings with splits etched at opposite ends [1]. However, depending on the requirements, a square-shaped or even a rectangular topology is convenient. For instance, rectangular SRRs have been used in microstrip lines loaded with these particles, since this topology enhances the coupling between the line and the rings [20, 21]. It has also been shown that chains of coupled SRRs etched in the same plane support magnetoinductive waves, but these structures exhibit a very narrow left-handed propagation band, unless rectangular SRRs with significant shape factors are considered (i.e. to enhance the inter-resonator's coupling, the SRRs must be much larger in the direction perpendicular to wave propagation) [36, 37]. In this work, we consider rectangular SRRs rather than circular ones. The reason is that, in the reported prototypes, these particles are either coupled to microstrip lines or directly coupled between them. SRR tunability is achieved by adding cantilever-type RF-MEMS switches, which are composed of one anchor and one movable beam suspended above an actuation electrode. We can combine SRRs and RF-MEMS in different configurations, as discussed below.

In configuration I (figure 1(a)), the external ring is used as a DC ground electrode and is the anchor for the

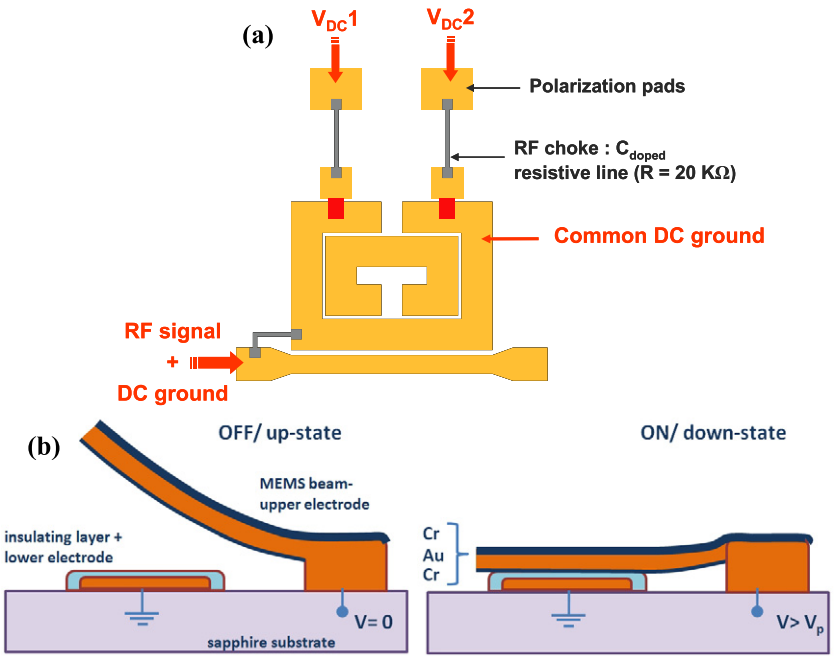

Figure 2. (a) DC actuation principle in the case of a SRR in configuration II, with two cantilever beams independently actuated. (b) Schematics and principle of operation of a fabricated electrostatic MEMS cantilever beam showing the two states: the non-actuated, up state (left-hand side) and the actuated, down state (right-hand side), when the applied voltage is higher than the MEMS pull-in voltage (Vp).

cantilever beams, while the internal ring, under them and covered by a thin dielectric layer, acts as the DC actuation electrode. When the cantilever beams are at the up state, the resulting capacitances formed with the internal ring are low. When they are actuated (down state), the coupling between rings dramatically increases and this leads to a very large shift of the resonance frequency of the resonator. In configuration II (figure 1(b)), the cantilever beam is anchored in a metallic patch and suspended over the outer ring. The switch actuation results in a resonance frequency decrement, and the frequency shift depends essentially on the metallic patch dimensions and location around the resonator. In configuration III (figure 1(c)), the cantilevers are also anchored in a metallic patch, which is placed inside the resonator, and suspended over the inner ring. Although prototypes based on this configuration are not provided in this paper, the simultaneous switch actuation results, in this case, in a frequency increase.

The previous configurations have been considered for the implementation of compact tunable metamaterial-based filters at the X-band. All the devices have been fabricated in a cleanroom environment using the same low-cost, batch and standard micro-fabrication process. Extensive details on fabrication and performances of similar MEMS actuators are described elsewhere [38, 39]. Briefly, the actuation electrodes are realized by the thermal evaporation of a Cr/Au (60/1200 Å) thin layer on a 250 μm thick sapphire substrate (with dielectric constant $\varepsilon_r = 9.8$). They are covered by a 0.4 μm thick Al_2O_3 dielectric layer deposited by plasma-enhanced chemical vapor deposition (PECVD). The alumina dielectric layer serves as an electrical insulator between the lower electrode (outer ring of the SRR structure) and the MEMS cantilever beam (the upper, moveable electrode, as shown in figure 2). It follows the lift-off of a 50 nm thick doped carbon layer, deposited by reactive laser ablation, to realize the 20 kΩ resistive lines. The suspended parts of the structure (moveable cantilever beam) are defined by patterning a 0.5 μm thick sacrificial PMGI resist. The metallization is done using the Cr/Au seed layer which is gold-electroplated up to 1.5 μm. Next, a 90 Å Cr stress layer is deposited and patterned, in order to provide an appropriate stress gradient in the foldable areas. Finally, the device is realized and dried in a critical point drying system to avoid stiction to the dielectric of the suspended structures.

As illustrated in figure 2 (corresponding to configuration II with the SRR coupled to a microstrip transmission line), the structure integrates carbon-doped resistive lines and metallic polarization pads for the electrostatic actuation of the RF-MEMS switches. Figure 2(b) shows the cross-sectional view (schematic) of the fabricated MEMS cantilever beams at both states. In order to carry out the electromagnetic characterization of the fabricated structures, they have been mounted in metallic boxes using SMA connectors. The performance of the fabricated tunable filters has been obtained by means of an Agilent 8710 network analyzer in the 1–20 GHz frequency range (the calibration used does not take into account losses induced by the SMA connectors).

3. Implementation of reconfigurable filters by means of MEMS-loaded SRRs

The combinations of SRRs and MEMS switches corresponding to configurations I and II of section 2 have been used for the implementation of electronically reconfigurable filters.

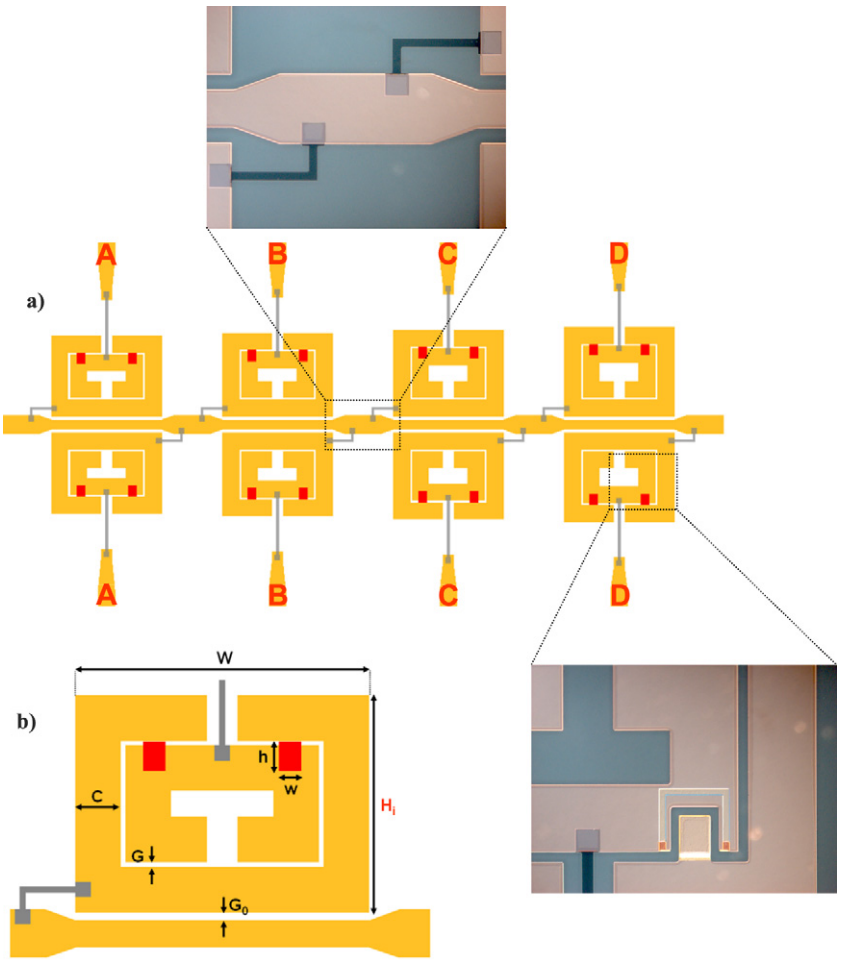

Figure 3. Layout of the all-integrated four-pole reconfigurable bandstop filter (a) and enlarged view of one RF-MEMS-loaded SRR (b). The total size of the device is 6.4 × 14 mm^2. The dimensions of the cantilever-type MEMS are $h \times w = 200 \times 150$ μm^2. Width and distance between rings are $C = 300$ μm and $G = 30$ μm. The gap between SRRs and the microstrip line is $G_0 = 50$ μm. The side length of the SRRs in the longitudinal direction is $W = 1940$ μm. Zoom photographs of the indicated parts of the fabricated device are also shown. Note that the right-hand side inset image is for a particular device for which the lower electrode is made of a conductive transparent layer (contour visible within the inner ring of the SRR).

Different types of filters, including stop band and band pass filters, have been designed and fabricated. Such filter prototypes are presented in this section. Filter bandwidth and/or central frequency are the tunable parameters of the proposed filters.

3.1. Stop band filter with electronically controllable numbers of poles (configuration I)

It is well known that transmission lines electrically or magnetically coupled to planar resonant elements exhibit transmission zeros at the resonance frequencies of the loading resonators [6, 21, 26]. At these frequencies, the resonators are driven by the line and the injected power is reflected back to the source. By loading the line with a single resonator, a notch in the transmission frequency, at the resonator's fundamental frequency and its harmonics, results. This is the principle for the implementation of notch filters, that is, filters exhibiting a very narrow stop band centered at the frequency to be suppressed. The bandwidth is related to the level of coupling and to the intrinsic (unloaded) quality factor of the considered resonator. The rejection level can be enhanced by adding particles resonating at the same frequency and uncoupled to the others (this inter-resonator's coupling must be avoided to circumvent the well-known split-off in the resonance frequency of coupled resonators). However, in many applications, the rejection bandwidth of the stop band filter must be broad. To this end, there are several approaches. One of them consists of loading the transmission line with multiple coupled resonators. Through Bloch mode analysis, it has been found that microstrip lines loaded with identical tightly coupled CSRRs exhibit a rejection band composed of an opaque region related to evanescent modes (in such a region signal propagation is inhibited due to the negative effective permittivity of the line) and a forbidden band related to the presence of complex modes (i.e. modes that are present as conjugate pairs, and hence they do not carry net power) [40]. The complex modes enhance the rejection band. However, in practice, the inter-resonator's coupling is limited and hence the rejection bandwidth is also limited.

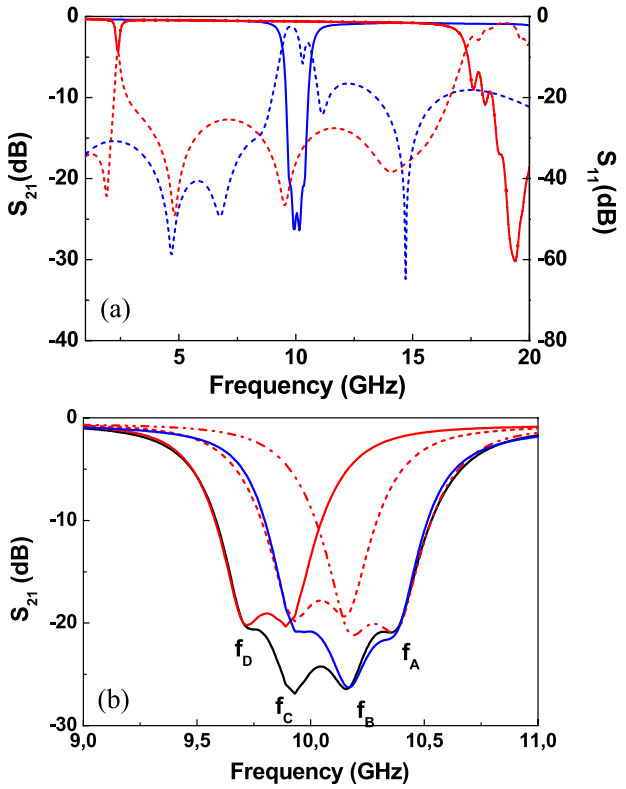

Figure 4. Simulated insertion (solid lines) and return (dotted lines) losses of the four-pole reconfigurable filter when all MEMS are at up state (blue) and all MEMS are at down state (red) (a). Simulated responses of the device for different combinations of switches actuated (b).

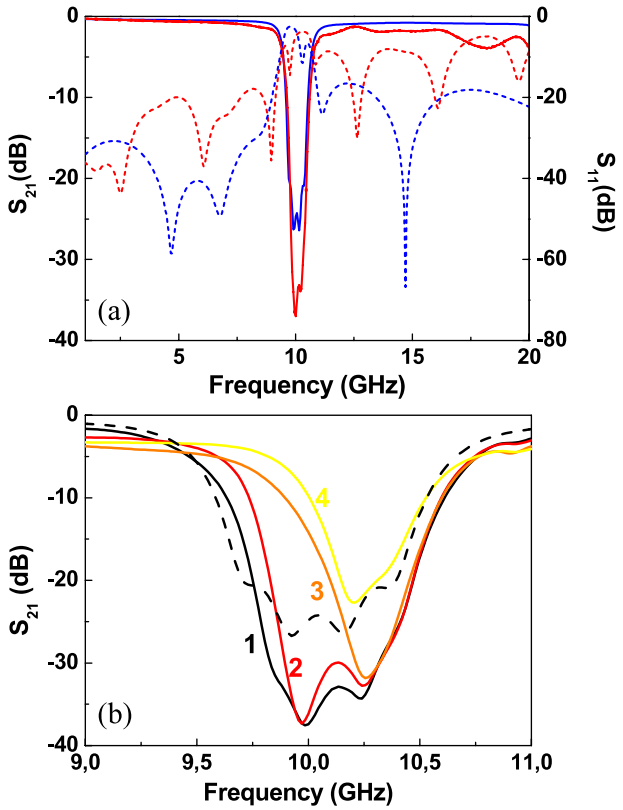

Figure 5. Simulated (blue) and measured (red) insertion (dashed lines) and return (dotted lines) losses of the four-pole reconfigurable stopband filter when all switches are at up state (a). Simulated (dashed line) and measured (solid lines) responses of the device for different combinations of switches actuated (b). Measurements indicated as 1, 2, 3 and 4 correspond to bits ABCD set to '0000', '0001', '0011' and '1011', respectively, with '0' corresponding to MEMS at up state (i.e. non-actuated) and '1' corresponding to MEMS at down state. Notice that the bit combinations of (b) do not have direct correspondence to those of figure 4(b), except for the cases '0000', '0001' and '0011'.

Another approach consists in loading the line with multiple resonators exhibiting slightly different frequencies within the required stop band. If the resonators are uncoupled, each resonator contributes with a filter pole (transmission zero) and bandwidth can be enhanced. This approach has been demonstrated in coplanar waveguides loaded with SRRs [41]. Due to the lack of periodicity, the stop band behavior cannot be interpreted in this case as due to effective media properties of the transmission line, but, from a practical viewpoint, the approach is very efficient (obviously, a combination of both strategies is also possible).

In the framework of the latter approach, i.e. multi-resonator coupling to the line, it is clear that filter characteristics can be tuned by removing one or more resonators (and hence the corresponding poles). In particular, we can modify the bandwidth and the central frequency and obtain different stop bands as well. However, by using MEMS switches in combination with SRRs according to configuration I, we can remove the poles without the need for resonator removal. We simply need to actuate the MEMS, and the pole (or poles) of the corresponding SRR will be largely shifted. Following this idea, we have designed a four-pole reconfigurable stop band filter (figure 3(a)). It consists of a 50 Ω microstrip transmission line loaded with four pairs of RF-MEMS-loaded SRRs. The difference between SRRs called A, B, C and D is the side length H_i of the external ring (figure 3(b)), where $H_A = 1430$ μm, $H_B = 1475$ μm, $H_C = 1530$ μm and $H_D = 1580$ μm. Without electrostatic actuation, this configuration provides a bandstop behavior with four poles corresponding to the resonance frequencies f_A (10.36 GHz), f_B (10.15 GHz), f_C (9.92 GHz) and f_D (9.73 GHz) of the SRRs of cells A, B, C and D, respectively (figure 4). The integration of the switching elements does not increase the dimensions of the structure. In contrast, the two capacitances formed by the cantilevers and the inner ring increase the coupling between rings, and this results in a decrease of the resonance frequency of the SRRs, and hence in an improvement of the electrical size of the particle. The area of each MEMS-loaded resonator is about $\lambda_g^2/32$, where λ_g is the guided wavelength at resonance. As shown in figures 3(a) and (b), the common DC ground signal is supplied to all external rings through the transmission line and resistive lines while each internal ring acts as a DC-independent electrode. The reconfigurable filter, designed to operate at the X-band, has been simulated by using the Agilent Momentum electromagnetic simulator. The ON/OFF RF-MEMS switches have been designed to provide a ratio between up-state and down-state capacitances of 10, which leads to a shift of the

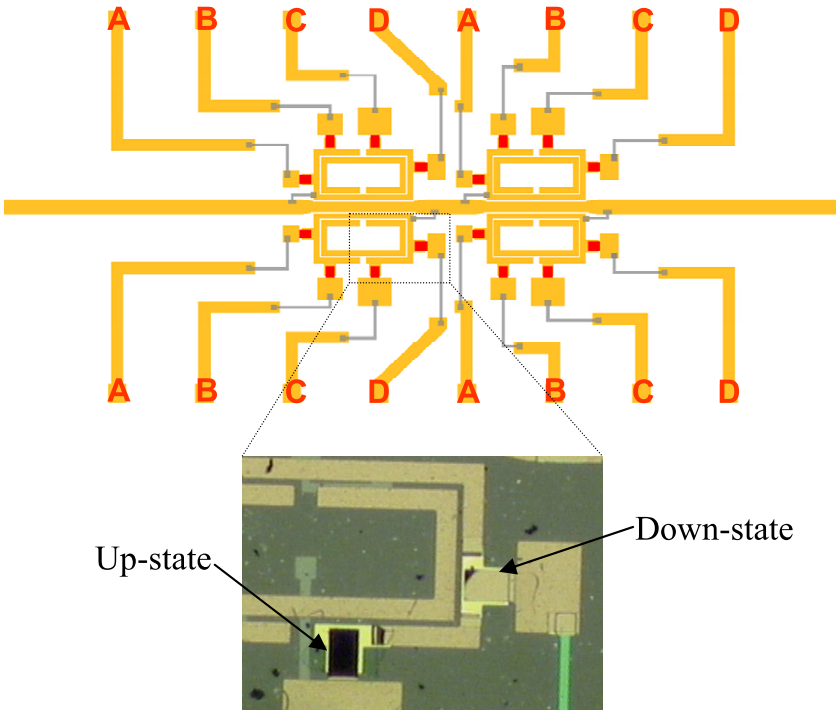

Figure 6. Layout of the all-integrated digitally tunable bandstop filter. The size of the active part of the device is 5.2×3.1 mm^2. The geometrical parameters illustrated in figure 3(b) are: $h \times w = 200 \times 150$ μm^2; $C = 100$ μm, $G = 20$ μm and $G_0 = 50$ μm; $W \times H = 1630 \times 830$ μm^2. A zoom photograph of the indicated part, with one MEMS switch in the up state and the other one in the down state, is also included (the non-actuated up-state switch exhibits a black color due to light contrast).

resonance frequencies of the resonators from the X-band to L-band.

Owing to the actuation of switches and taking into account that both SRRs of one cell must always present the same resonance frequency, we obtain a four-bit (called A, B, C and D) reconfigurable filter. The simulated S parameters of the device are displayed in figure 4(a). When all switches are at up state, the rejection is higher than 20 dB in a 0.7 GHz range. When they are all at down state, insertion losses are less than 1 dB and return losses higher than 20 dB in a range from 3 to 16 GHz. The curves in figure 4(b) present other simulated filter responses corresponding to different bit combinations. By varying the number of switches actuated, we can digitally tune the filter bandwidth and central frequency.

The measured insertion and return losses of the filter with all MEMS at up state (non-actuated) are presented in figure 5(a) and compared with the full wave simulations. As expected, the filter exhibits a four-pole rejection band around 10 GHz and the rejection is higher than 20 dB on a 0.72 GHz frequency range. There is good agreement between simulation and experiment, except that out of the stop band measured insertion losses are higher and return losses are lower than those predicted by the simulation. This is due to the connection between the transmission line of the filter and the two SMA connectors. Other measured filter responses corresponding to different combinations of switches simultaneously actuated by 60 V are depicted in figure 5(b). The number of poles of the stop band corresponds to the number of non-actuated switches. The digital reconfigurability principle is hence validated.

3.2. Stop band filter based on digitally tunable resonators (configuration II)

In the filter reported in section 3.1, the reconfigurability was achieved by canceling the effects of the coupled resonators by means of MEMS actuation (i.e. by shifting the corresponding poles outside the region of interest). Let us now consider a different tuning principle based on configuration II. The proposed filter is an X-band digitally tunable stop band filter depicted in figure 6. It consists on a microstrip line loaded with two pairs of identical SRRs. Each SRR is loaded with four MEMS switches, which can be independently actuated. As shown in figure 6, the common DC ground signal is supplied to all externals rings through the transmission line and resistive lines, while each metallic patch, acting as the anchor of the cantilever beam, acts also as its DC-independent electrode. The tuning principle is very simple: by independently actuating on the MEMS switches of each SRR, the corresponding resonance frequency can be digitally controlled. Therefore, we can control the central filter frequency or the bandwidth. If the same combination of MEMS actuation is applied to the four SRRs, the central frequency can be digitally tailored. However, if different combinations of actuating voltages are applied to the different SRRs, different poles are generated, and both the central frequency and bandwidth can be controlled. The dimensions and the position of the metallic patches around the resonators have been optimized to obtain a total resonance frequency shift of 1.5 GHz with regular steps of 0.1 GHz. Figure 7 depicts the simulated frequency response of the filter with

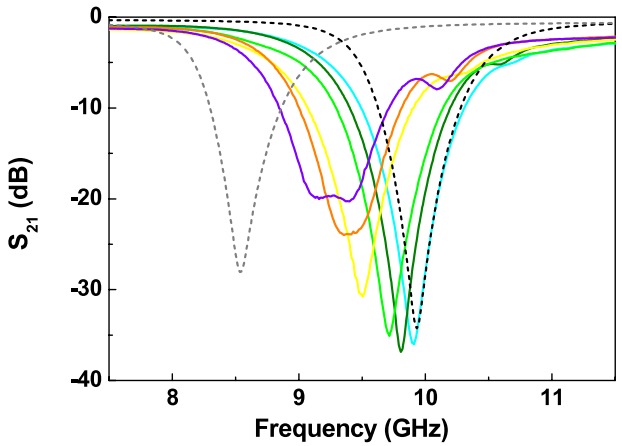

Figure 7. Measured (colored solid lines) and simulated (dashed curves) responses of the digitally tunable bandstop filter for different combinations of switches actuated. Notice that the experimental frequency response corresponding to all switches actuated has been omitted since some switches do not respond to the actuation voltages for unknown reasons.

all switches actuated and with all switches non-actuated. As mentioned before, the central frequency is shifted down by 1.5 GHz when all MEMS are at down state. We have also obtained several measurements corresponding to different combinations of MEMS actuated (including different combinations for different SRRs). The results illustrate the flexibility of the proposed approach to digitally tune the filter frequency response.

3.3. Digitally tunable band pass filter (configuration II)

The RF-MEMS-loaded SRRs of configuration II have also been used for the design of a tunable band pass filter. The topology, depicted in figure 8, consists of a pair of coupled SRRs fed by 50 Ω microstrip transmission lines. In the proposed configuration, the electrical coupling between these two adjacent elements results in the band pass behavior of the filter [42]. Such a configuration provides also transmission zeros, present on both sides of the band, which are relevant for frequency selectivity improvement and are caused by the feeding structure, as discussed in [43]. Since the central frequency of the filter depends directly on the resonance frequency of the SRRs, by tuning the SRRs we can tailor the position of the filter pass band. On the other hand, bandwidth is mainly controlled by the coupling level between SRRs, which is scarcely dependent on MEMS actuation. Therefore, the proposed tunable filters are specifically designed to tune the central filter frequency. For the un-tuned state (non-actuated MEMS), there is a systematic approach for the design of these types of filters. That is, given filter specifications (bandwidth, order, central frequency and minimum return in-band losses), the inter-resonator coupling coefficients and external quality factors are determined and, from these values, the inter-resonator's distance as well as the position of the feeding lines are determined [44]. However, since the main relevant aspect of this work is to highlight novel tuning concepts for filter design based on RF-MEMS switches, rather than pursuing a specific frequency response, we have tuned the inter-resonator's distance in order to obtain a filter response with a fractional bandwidth (non-actuated switches) of roughly 15%. In order to improve the frequency selectivity of the filter, rather than considering a symmetric topology, we have used a skew symmetric 0° feed configuration, as reported in [43]. This produces one transmission zero at each side of the pass band, at those frequencies where the two signal paths between the feed point and the edges of the external ring, are about one-quarter wavelength.

The dimensions of the metallic patches to which the RF-MEMS are anchored determine the tuning range. The designed prototype has been merely fabricated as a proof of concept; hence the metallic patches have been chosen with arbitrary dimensions. The measured frequency responses corresponding to four different states are depicted in figure 9. We note that this fabricated device has not been mounted on a metallic box with SMA connectors like the other devices presented in this paper, but on a thick dielectric substrate, and the transmission line is connected by wire bonding to

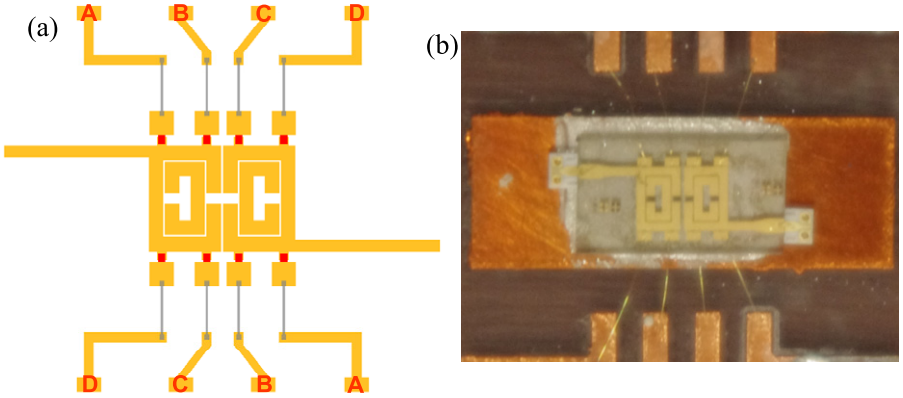

Figure 8. (a) Layout of the four-bit tunable bandpass filter. The geometrical parameters illustrated in figure 3(b) are: $h \times w = 200 \times 150\ \mu m^2$; $C = 300\ \mu m$, $G = 30\ \mu m$ and $W \times H = 2190 \times 1490\ \mu m^2$. (b) Photograph of the fabricated device where the MEMS switches are fed through wire bonding.

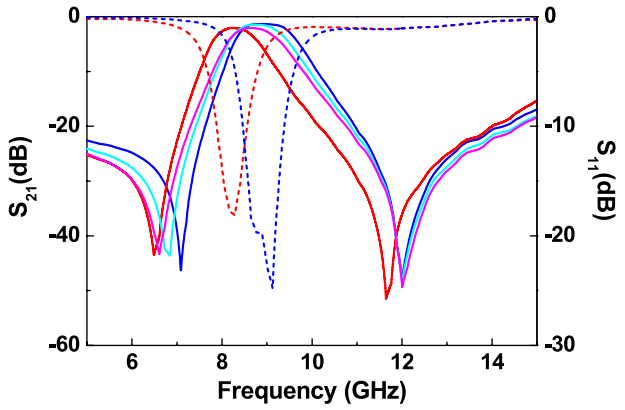

Figure 9. Measured insertion (solid line) and return (dashed line) losses of the designed digitally tunable bandpass filter for four different switching states. The switching states are: '0000' (dark blue), '0001' (pale blue), '0011' (pink) and '1111' (red), where the bit sequence is for switches ABCD, and '0' and '1' stand for non-actuated and actuated, respectively.

a commercial microstrip to coplanar transitions to make RF measurements. The responses at the two extremes correspond to all switches on and off. From this, the tuning range is found to be roughly 10%. Filter performance is good, with measured in-band insertion losses (central frequency) of 1.3 and 2 dB at the two extremes of the tuning range, and return losses better than 35 dB in both cases. It is found that MEMS actuation does also shift down the transmission zero frequencies.

4. Conclusions

In conclusion, it has been demonstrated that split ring resonators (SRRs) can be combined with RF-MEMS switches in order to implement electronically tunable resonant elements. Different configurations of MEMS-loaded SRRs have been considered and applied to the design of tunable stop band filters and band pass filters. The reported stop band filters are microstrip lines loaded with the tunable resonant elements, whereas the designed band pass filter has been implemented by coupling two tunable SRR. In all cases, the tuning principle has been the control of the resonance frequency of the involved resonators through MEMS switch actuation. The reported structures exhibit reasonable characteristics (in good agreement with the full wave electromagnetic simulations) and are compact. With the fabricated prototypes, the application of RF-MEMS technology to the design of metamaterial-inspired tunable microwave filters is validated.

Acknowledgments

This work has been supported by the Spanish projects CSD2008-00066, TEC2010-17512 and SGR2009-421.

References

[1] Pendry J B, Holden A J, Robbins D J and Stewart W J 1999 Magnetism from conductors and enhanced nonlinear phenomena *IEEE Trans. Microw. Theory Tech.* **47** 2075–84

[2] Smith D R, Padilla W J, Vier D C, Nemat-Nasser S C and Schultz S 2000 Composite medium with simultaneously negative permeability and permittivity *Phys. Rev. Lett.* **84** 4184–7

[3] Falcone F, Lopetegi T, Baena J D, Marqués R, Martín F and Sorolla M 2004 Effective negative-ε stop-band microstrip lines based on complementary split ring resonators *IEEE Microw. Wireless Compon. Lett.* **14** 280–2

[4] Falcone F, Lopetegi T, Laso M A G, Baena J D, Bonache J, Marqués R, Martín F and Sorolla M 2004 Babinet principle applied to the design of metasurfaces and metamaterials *Phys. Rev. Lett.* **93** 197401

[5] Baena J D, Marqués R, Medina F and Martel J 2004 Artificial magnetic metamaterial design by using spiral resonators *Phys. Rev.* B **69** 014402

[6] Falcone F, Martín F, Bonache J, Laso M A G, García-García J, Baena J D, Marqués R and Sorolla M 2004 Stop band and band pass characteristics in coplanar waveguides coupled to spiral resonators *Microw. Opt. Technol. Lett.* **42** 386–8

[7] Bilotti F, Toscano A, Vegni L, Aydin K, Alici K B and Ozbay E 2007 Equivalent-circuit models for the design of metamaterials based on artificial magnetic inclusions *IEEE Trans. Microw. Theory Tech.* **55** 2865–73

[8] Bilotti F, Toscano A and Vegni L 2007 Design of spiral and multiple split-ring resonators for the realization of miniaturized metamaterial samples *IEEE Trans. Antennas Propag.* **55** 2258–67

[9] Rogacheva A V, Fedotov V A, Schwanecke A S and Zheludev N I 2006 Giant gyrotropy due to electromagnetic-field coupling in a bilayered chiral structure *Phys. Rev. Lett.* **97** 177401

[10] Marqués R, Jelinek L and Mesa F 2006 Negative refraction from quasi-planar chiral inclusions *Microw. Opt. Technol. Lett.* **49** 2606–9

[11] Martel J, Marqués R, Falcone F, Baena J D, Medina F, Martín F and Sorolla M 2004 A new LC series element for compact band pass filter design *IEEE Microw. Wireless Compon. Lett.* **14** 210–2

[12] Velez A, Aznar F, Bonache J, Velázquez-Ahumada M C, Martel J and Martín F 2009 Open complementary split ring resonators (OCSRRs) and their application to wideband CPW band pass filters *IEEE Microw. Wireless Compon. Lett.* **19** 197–9

[13] Erentok A, Luljak P L and Ziolkowski R W 2005 Characterization of a volumetric metamaterial realization of an artificial magnetic conductor for antenna applications *IEEE Trans. Antennas Propag.* **53** 160–72

[14] Ozbay E, Aydin K, Butun S, Kolodziejak K and Pawlak D 2007 Ferroelectric based tuneable SRR based metamaterial for microwave applications *2007 European Microwave Conf.* 497–9

[15] Gil M, Damm C, Giere A, Sazegar M, Bonache J, Jakoby R and Martín F 2009 Electrically tunable split-ring resonators at microwave frequencies based on Barium–Strontium Titanate thick-film *Electron. Lett.* **45** 417–9

[16] Bouyge D, Crunteanu A, Orlianges J-C, Passerieux D, Champeaux C, Catherinot A, Velez A, Bonache J, Martin F and Blondy P 2009 Reconfigurable bandpass filter based on split ring resonators and vanadium dioxide (VO_2) microwave switches *Asia-Pacific Microwave Conf.* 2332–5

[17] Padilla W J, Taylor A J, Highstrete C, Lee M and Averitt R D 2006 *Phys. Rev. Lett.* **96** 107401

[18] Gökkavas M, Güven K, Bulu I, Aydin K, Penciu R S, Kafesaki M, Soukoulis C M and Ozbay E 2006 *Phys. Rev.* B **73** 193103

[19] Gundogdu T F, Gökkavas M, Güven K, Kafesaki M, Soukoulis C M and Ozbay E 2007 Simulation and

micro-fabrication of optically switchable split ring resonators *Photon. Nanostruct.—Fundam. Appl.* **5** 106–12
[20] Gil I, Martin F, Bonache J and Garcia-Garcia J 2006 Tunable metamaterial transmission lines based on varactor loaded split rings resonators *IEEE Trans. Microw. Theory Tech.* **54** 2665–74
[21] Gil I, Garcia-Garcia J, Bonache J, Martin F, Sorolla M and Marques R 2004 Varactor-loaded split rings resonators for tunable notch filters at microwave frequencies *Electron. Lett.* **40** 1347–8
[22] Yongxuan X, Donglin S, Yazhou W and Yan Z 2006 The laminating tunable notch filter with single split ring resonator *2006 4th Asia-Pacific Conf. on Environmental Electromagnetics* 465–7
[23] Li H, Zhang Y and He L 2008 Tunable filters based on the varactor-loaded split-ring resonant structure coupled to the microstrip line *2008 Int. Conf. on Microwave and Millimeter wave Technology* 1580–2
[24] Aydin K and Ozbay E 2007 Capacitor-loaded split ring resonators as tunable metamaterial components *J. Appl. Phys.* **101** 024911
[25] Lopez M A, Freire M J, Algarin J M, Behr V C, Jakob P M and Marques R 2011 Nonlinear split-ring metamaterial slabs for magnetic resonance imaging *Appl. Phys. Lett.* **98** 133508
[26] Vélez A, Bonache J and Martín F 2008 Varactor-loaded complementary split ring resonators (VLCSRR) and their application to tunable metamaterial transmission lines *IEEE Microw. Wireless Compon. Lett.* **18** 28–30
[27] Lacroix B, Pothier A, Crunteanu A, Cibert C, Dumas-Bouchiat F, Champeaux C, Cathérinot A and Blondy P 2007 Sub-microsecond RF MEMS switched capacitors *IEEE Trans. Microw. Theory Tech.* **55** 1314–21
[28] Lakshminarayanan B, Mercier D and Rebeiz G 2008 High-reliability miniature RF-MEMS switched capacitors *IEEE Trans. Microw. Theory Tech.* **56** 971–81
[29] Papaioannou G J and Papapolymerou J 2007 Dielectric charging mechanisms in RF-MEMS capacitive switches *37th European Microwave Conf. Proc. (Munich)* 359–62
[30] Young R M *et al* 2003 Low-loss bandpass RF filter using MEMS capacitance switches to achieve a one-octave tuning range and independently variable bandwidth *IEEE MTT Int. Microwave Symp. Dig.* **3** 1781–4
[31] Papapolymerou J *et al* 2003 Reconfigurable double-stub tuners using MEMS switches for intelligent RF front-ends *IEEE Trans. Microw. Theory Tech.* **51** 272–8
[32] Gil I, Martin F, Rottenberg X and De Raedt W 2007 Tunable stop-band filter at Q-band based on RF-MEMS metamaterials *Electron. Lett.* **43** 1153–4
[33] Hand T and Cummer S 2007 Characterization of tunable metamaterial elements using MEMS switches *IEEE Antennas Wireless Propag. Lett.* **6** 401–4
[34] Tao H, Strikwerda A C, Fan K, Padilla W J, Zhang X and Averitt R D 2011 MEMS based structurally tunable metamaterials at terahertz frequencies *J. Infrared Millim. Terahz. Waves* **32** 580–95
[35] Bouyge D, Mardivirin D, Bonache J, Crunteanu A, Pothier A, Durán-Sindreu M, Blondy P and Martín F 2011 Split ring resonators (SRRs) based on micro-electro-mechanical deflectable cantilever-type rings: application to tunable stopband filters *IEEE Microw. Wireless Compon. Lett.* **21** 243–5
[36] Syms R R A, Shamonina E, Kalinin V and Solymar L 2005 A theory of metamaterials based on periodically loaded transmission lines: interaction between magnetoinductive and electromagnetic waves *J. Appl. Phys.* **97** 064909
[37] Freire M J, Marqués R, Medina F, Laso M A G and Martín F 2004 Planar magneto-inductive wave transducers: theory and applications *Appl. Phys. Lett.* **85** 4439–41
[38] Mardivirin D, Pothier A, Crunteanu A, Vialle B and Blondy P 2009 Charging in dielectric less capacitive RF-MEMS switches *IEEE Trans. Microw. Theory Tech.* **57** 231–6
[39] Fabert M, Desfarges-Berthelemot A, Kermène V, Crunteanu A, Bouyge D and Blondy P 2008 Ytterbium-doped fibre laser Q-switched by a cantilever-type micro-mirror *Opt. Express* **16** 22064–71
[40] Tamir T and Oliner A A 1963 Guided complex waves *Proc. IEEE* **110** 310–34
[41] Martín F, Falcone F, Bonache J, Lopetegi T, Marqués R and Sorolla M 2003 Miniaturized CPW stop band filters based on multiple tuned split ring resonators *IEEE Microw. Wireless Compon. Lett.* **13** 511–3
[42] Hong J-S and Lancaster M J 1996 Couplings of microstrip square open-loop resonators for cross-coupled planar microwave filters *IEEE Trans. Microw. Theory Tech.* **44** 2099–109
[43] Tsai C-M, Lee S-Y and Tsai C-C 2002 Performance of a planar filter using a 0° feed structure *IEEE Trans. Microw. Theory Tech.* **50** 2362–7
[44] Hong J-S and Lancaster M J 2001 *Microstrip Filters for RF/Microwave Applications* (New York: Wiley)